RESEARCH ARTICLE

# Regulation of glioma cell invasion by 3q26 gene products PIK3CA, SOX2 and OPA1

Thorsten Schaefer[2,*]; Archana Ramadoss[1,*]; Severina Leu[4,*]; Lionel Tintignac[3]; Cristobal Tostado[1]; Andrea Bink[7,8] (iD) ; Christoph Schürch[2]; Joëlle Müller[2]; Jonas Schärer[2]; Giusi Moffa[6] (iD) ; Philippe Demougin[9]; Suzette Moes[10]; Christoph Stippich[7,8]; Simona Falbo[1]; Heike Neddersen[4]; Heiner Bucher[6]; Stephan Frank[5]; Paul Jenö[10]; Claudia Lengerke[2,11]; Marie-Françoise Ritz[1]; Luigi Mariani[1,4,†]; Jean-Louis Boulay[1,†] (iD)

1 Laboratory of Brain Tumor Biology, Department of Biomedicine, University Hospital and University of Basel, Basel, Switzerland.
2 Stem Cells and Hematopoiesis Laboratory, Department of Biomedicine, University Hospital and University of Basel, Basel, Switzerland.
3 Neuromuscular Research Laboratory, Department of Biomedicine, University Hospital and University of Basel, Basel, Switzerland.
4 Neurosurgery Clinic, University Hospital and University of Basel, Basel, Switzerland.
5 Division of Neuropathology, University Hospital and University of Basel, Basel, Switzerland.
6 Basel Institute for Clinical Epidemiology and Biostatistics, University Hospital and University of Basel, Basel, Switzerland.
7 Department of Neuroradiology, University Hospital and University of Basel, Basel, Switzerland.
8 Clinic for Neuroradiology, University Hospital Zurich, University of Zurich, Zurich, Switzerland.
9 Life Sciences Training Facility, University of Basel, Basel, Switzerland.
10 Proteomics Core Facility, Biozentrum, University of Basel, Basel, Switzerland.
11 Division of Hematology, University Hospital Basel, Basel, Switzerland.

## Abstract

Diffuse gliomas progress by invading neighboring brain tissue to promote postoperative relapse. Transcription factor *SOX2* is highly expressed in invasive gliomas and maps to chromosome region 3q26 together with the genes for PI3K/AKT signaling activator PIK3CA and effector molecules of mitochondria fusion and cell invasion, MFN1 and OPA1. Gene copy number analysis at 3q26 from 129 glioma patient biopsies revealed mutually exclusive *SOX2* amplifications (26%) and *OPA1* losses (19%). Both forced *SOX2* expression and *OPA1* inactivation increased LN319 glioma cell invasion *in vitro* and promoted cell dispersion *in vivo* in xenotransplanted *D. rerio* embryos. While PI3 kinase activity sustained SOX2 expression, pharmacological PI3K/AKT pathway inhibition decreased invasion and resulted in SOX2 nucleus-to-cytoplasm translocation in an mTORC1-independent manner. Chromatin immunoprecipitation and luciferase reporter gene assays together demonstrated that SOX2 *trans*-activates *PIK3CA* and *OPA1*. Thus, SOX2 activates PI3K/AKT signaling in a positive feedback loop, while *OPA1* deletion is interpreted to counteract *OPA1 trans*-activation. Remarkably, neuroimaging of human gliomas with high *SOX2* or low *OPA1* genomic imbalances revealed significantly larger necrotic tumor zone volumes, corresponding to higher invasive capacities of tumors, while autologous necrotic cells are capable of inducing higher invasion in *SOX2* overexpressing or *OPA1* knocked-down relative to parental LN319. We thus propose necrosis volume as a surrogate marker for the assessment of glioma invasive potential. Whereas glioma invasion is activated by a PI3K/AKT-SOX2 loop, it is reduced by a cryptic invasion suppressor SOX2-OPA1 pathway. Thus, PI3K/AKT-SOX2 and mitochondria fission represent connected signaling networks regulating glioma invasion.

## INTRODUCTION

Diffuse gliomas are among the most aggressive human tumors. Glioblastoma (GB), the most malignant form of glioma either develops *de novo*, or from the progression of lower grade glioma (LGG). Currently, surgical resection and chemotherapy remain the standard therapies, although they are not curative, and have limited prognostic impact (22,31).

Unlike tumors of other tissue lineages, which are prone to metastasize into remote organs, diffuse gliomas progress by tumor cell invasion into adjacent healthy brain regions, which almost invariably gives rise to tumor recurrence. Thus, identification of molecular mechanisms underlying glioma cell invasion is an important goal toward improving glioma patient survival.

Glioma cells detach from the bulk of the tumor mass by losing adhesion, gaining motility and progress by interaction with extracellular matrix (ECM) and surrounding tissue. Migratory routes are either perivascular, or within the brain parenchyma (7,12,27). Among the known molecular mechanisms that regulate effectors of glioma invasion, TGF-ß activates expression of matrix metalloproteinase-2 (MMP-2), as well as of the transcription factors Snail, Twist and ZEB family members. As a consequence, glioma cells undergo an epithelial-to-mesenchymal transition (EMT), a precursor state of invasive behavior (20,36,41). The PI3K/AKT pathway, activated by receptor tyrosine kinase signaling or PTEN loss, increases the activity of MMP-2 and MMP-9, while Notch signaling *trans*-activates the ECM protein tenascin-C (32). Further adding to these aspects, we find here *SOX2* transcripts associated with higher invasion in LGG (data shown in Supplementary Figure S1). SOX2 is known to maintain glioma cell stemness, for driving EMT in many solid tumors (14,21,23,26,42) and for inducing cell invasion (2,3,13,35). SOX2 is induced

by TGF-ß *via* SOX4 and activates the Notch pathway to mediate tenascin-dependent glioma cell invasion (16,32,43).

*SOX2* maps to chromosome band 3q26, which is known for frequent genetic imbalances in gliomas (25). Not surprisingly, this region contains several genes with potential or proven impact on tumor development (Figure 1A). Among them *PIK3CA*, which encodes p110α, the catalytic subunit of the predominant form of PI3 kinase, and thus is a key constituent of the canonical PI3K/AKT signaling axis. PIK3CA carries gain-of-function missense mutations in about 10% of GB, at the same hotspots as observed in other cancers (29). For example, in mammary carcinoma, where activating *PIK3CA* mutations are recurrent hits and the PI3K/AKT signaling pathway shown to sustain SOX2 nuclear expression, more specifically (25,30,34). Further relevant genes encoded on 3q26 comprise *OPA1* and *MFN1*. Germline mutations in the *OPA1* (optical atrophy 1) gene are responsible for autosomal dominant optic atrophy. *OPA1*, together with the mitofusin-1 gene *MFN1*, are both involved in mitochondrial fusion (9,33). Of interest,
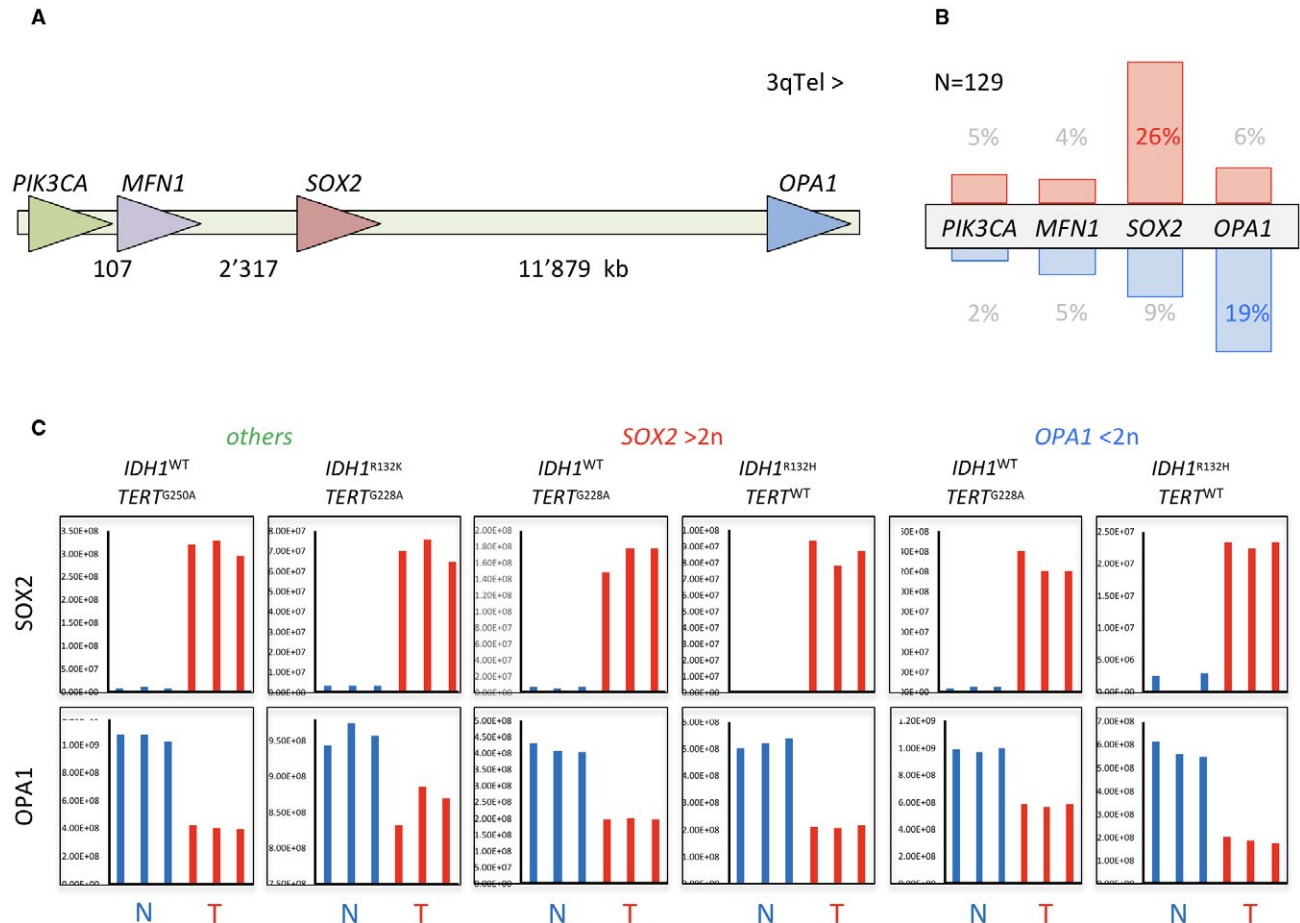


**Figure 1.** 3q26 genes *SOX2* and *OPA1* are targeted in glioma. A. Schematic illustration of chromosome segment 3q26 with indication of relative position and orientation of *PIK3CA, MFN1, SOX2* and *OPA1* genes. B. Frequency of genomic amplification (red) and deletion (blue) of 3q26 genes as determined by quantitative PCR of DNA from 129 glioma biopsies. C. Protein levels of SOX2 and OPA1 determined by mass spectrometry in six representative glioma biopsies (T) compared with corresponding non-tumorous white matter (N). The glioma biopsies were genotyped to be either *IDH* wild type or mutant, or carrying *SOX2* amplification (*SOX2 > 2n*) or *OPA1* deletion (*OPA1 < 2n*). "*Others*" stands for glioma with neither *SOX2* amplification nor *OPA1* deletion.

mitochondrial fission has been associated with cell polarization and an increased cell motility of lymphocytes as well as breast and thyroid cancer cells (4,10,11). Therefore, given the vicinity of these genes in the human genome, we hypothesized that they could interact with SOX2 to result in enhanced cell invasion.

Neuroimaging parameters allow detection and measurement of distinct compartments of tumor anatomy of potential diagnostic or prognostic value (38). T2w-hyperintense non-enhancing domains represent the tumor parts of lower grade with intact blood-brain barrier (BBB) (19,44). Breakdown of BBB, an indicator for malignancy, allows contrast uptake and gives brightness to contrast-enhanced T1-weighted images. Measurement of contrast-enhancing tumor by response assessment to neuro-oncology (RANO) expresses—as one part of this assessment—the largest area of tumor extension in axial direction (39). The necrosis compartment, usually embedded in the enhancing volume, can be triggered by tumor necrosis factor secreted by glioma cells (28). Necrosis is a hallmark of GB, a survival marker and inducer of glioma cell invasion (1,15,44). As exemplified in Figure 6A, these three compartments represent altogether the neuroradiologically visible total volume of the tumor with invading glioma cells spreading far beyond the visible boundaries.

We here describe that molecular interactions between 3q26 gene products SOX2, PIK3CA and OPA1 combined with respective gene copy imbalances determine glioma invasion capacity in cell-based *in vitro* assays and xenotransplant *in vivo* studies alike. These molecular findings meet a phenotypic manifestation in human gliomas, whose neuro radiologic examination revealed that tumors with *SOX2* amplification or *OPA1* deletion had larger volumes of tumor necrosis, an established inducer of invasion.

# MATERIALS AND METHODS

## Cell culture, lentiviral transduction and plasmid transfection

Human glioma LN319 (17) and human embryonic kidney HEK293 cells (ATCC #CRL-1573) were grown in Dulbecco's modified Eagle's medium (DMEM, Sigma-Aldrich, #D6429) supplemented with 5% heat-inactivated fetal bovine serum (Sigma-Aldrich, #F7524) and 1% Pen/Strep (Sigma-Aldrich, #P4333). Short-term *ex vivo* cell cultures derived from dissociated patient tumor tissue were grown in DMEM supplemented with 30mM Hepes, 10% fetal bovine serum and 1% Pen/Strep.

A *mCherry* color reporter was N-terminally fused to human *SOX2* cDNA, inserted into a pLVX-puro expression vector (Clontech, Mountain View, CA, USA) and stably integrated into LN319 cells by lentiviral transduction. Expression of the corresponding fusion protein was driven from a doxycycline-dependent (D9891, Sigma, St-Louis, MO, USA) TetON gene induction system as described (30). Integrants were positively selected first by puromycin resistance and subsequently by FACS. $PIK3CA^{WT}$, $PIK3CA^{H1047R}$ and $PIK3CA^{E545K}$ constructs encoding HA-tagged variants of the catalytic subunit of PI3 kinase alpha p110α were PCR-amplified from Addgene plasmids #12522, #12524, and #12525, *Bam*HI-inserted into pLVX-puro, and likewise lentivirally integrated into LN319 and expressed in doxycycline-inducible manner. Lentiviruses expressing shRNA against *OPA1* and scrambled control (Santa Cruz Biotechnology #sc-106808-V, #sc-108080-V Dallas, TX, USA) were transduced into LN319 cells according to the manufacturer's instructions and positively selected with puromycin (Sigma-Aldrich, #P8833). HEK293 cells were transfected using reagent JET PEI™ (Polypus-transfection #101-01N; ArchiMed, Lyon, France).

## Nucleic acid extraction and analysis

RNA from cell cultures was extracted using Trizol (Thermo Fischer Scientific #15596-026) and RNeasy Mini Kit (Qiagen #74104; Hombrechtikon, Switzerland). Reverse transcription was performed with iScript cDNA Synthesis Kit (Bio-Rad #170-8890). Quantitative PCR was performed with Ssofast Evagreen supermix (Bio-Rad #172-5200) using the CFX90 thermocycler (Bio-Rad, Hercules, CA, USA). Samples were normalized with *GAPDH*. Primers for cDNAs were purchased from Qiagen, and where *PIK3CA*: QT000114861, *SOX2*: QT00237601, *MFN1*: QT00077966, *OPA1*: QT00085519 and *GAPDH*: QT00079247. Genomic DNA from glioma biopsies was extracted using DNeasy Blood & Tissue Kit (Qiagen, Cat # 69504). Forward (F) and reverse (R) primers for copy number variation studies were: *PIK3CA* (F: gag aaa atg aaa gct cac tct gg and R: gtg cta tca aac cct gtt tgc, *SOX2* (F: tga gag aga tcc tgg act tc and R: gca aac ttc ctg caa agc tc), *MFN1* (F: gcc tcc tga aga aca aca gc and R: agg aac gct ttc cta gtg ca), *OPA1* (F: cac tga ttt cct tga gtt ctc a and R: act gtt tgg ggt tga tat ttg g), *IDH1* (F: *acc aaa tgg cac cat acg a* and R: *ttc ata cct tgc tta atg ggt gt*).

## Western blotting and immunodetection

Cells were disrupted in 1x lysis buffer (#9803, Cell Signaling, Danvers, MA, USA) supplemented with protease and phosphatase inhibitors (#78442, Thermo Fisher Scientific, Waltham, MA, USA). Total cell lysates were cleared at 4°C for 10 minutes at 15 000 rpm and supplemented with Laemmli buffer. Alternatively (Figure 2B), cell lysates were extracted using the NE-PER kit (Thermo Fischer Scientific #78833).

Proteins were separated on Novex PAGE gels (Invitrogen, Carlsbad, CA, USA) and transferred onto PVDF membrane (#10600021, Amersham, GE Healthcare Life Sciences, Chalfont St. Giles, UK) in a semi-dry blotting apparatus (Trans-Blot Turbo, BioRad). Membranes were blocked with 10% w/v nonfat dry milk (#9999S, Cell Signaling) diluted in TBS containing 0.1% Tween-20 (P1379, Sigma). Proteins were decorated with the following primary antibodies: anti PI3 kinase p110α (Cell Signaling Technology (CST), #4255), pAKT(Ser473) (CST, #4060), AKT (CST, #4691), SOX2 (CST, #3579), pRPS6(Ser235,Ser236) (CST, #4856), actin (CST, #3700) and detected by ECL reaction.
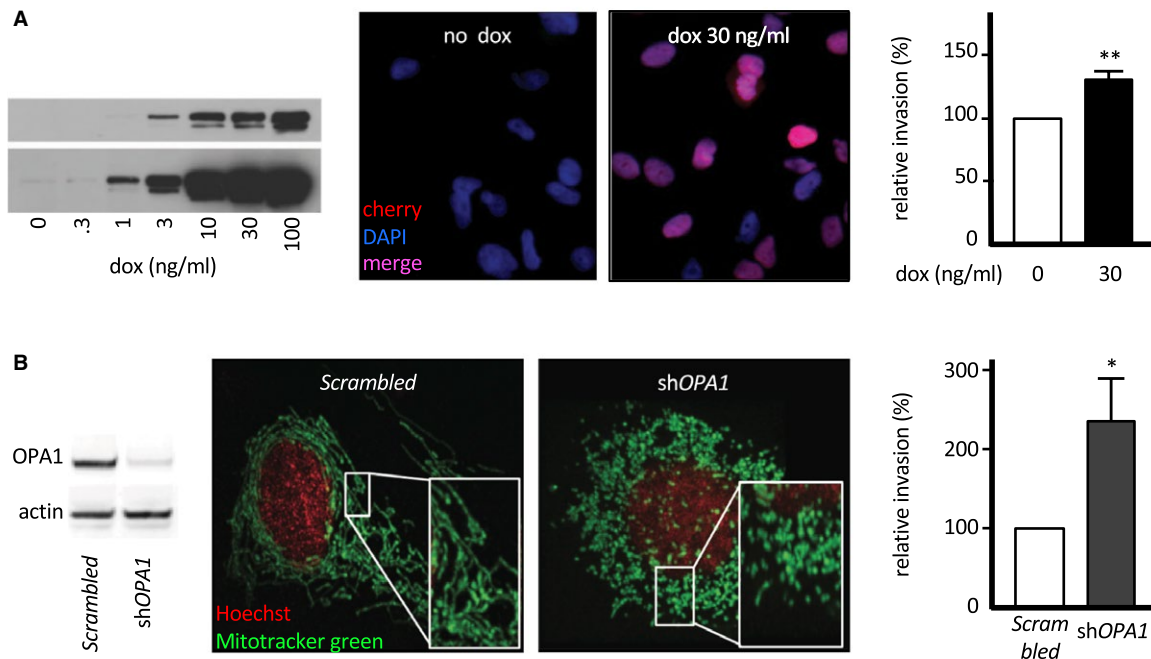
**Figure 2.** SOX2 and OPA1 modulate glioma cell invasion *in vitro* and *in vivo*. **A.** Inducible SOX2 overexpression in LN319 cells. LN319 stably transfected with an mCherry-SOX2 fusion construct under control of a doxycycline-inducible promoter. Western blot documenting dose-dependent induction of the fusion protein (anti-SOX2 staining, two exposure times, left). Fluorescence microscopy verifying effective nuclear localization of mCherry-SOX2 24 h past induction (middle).

SOX2-dependent modulation of cell invasiveness as investigated by 24 h Boyden chamber assay (right). **B.** shRNA-driven *OPA1* knock-down in LN319 cells. Western blot of transfected LN319 cells (left). Verification of knock-down phenotype by mitochondria morphology in transfected LN319 (middle). Comparative cell invasion in response by 24 h Boyden chamber assay (right).

For immunofluorescence, cells were fixed with 4% formaldehyde for 10 minutes followed by permeabilization with 0.2% Tween in blocking buffer (PBS + 5% normal serum). Cells were incubated overnight with anti-SOX2 (Millipore #MAB4343) then with Cy2-conjugated secondary antibodies (Jackson ImmunoResearch, Cambridgeshire, UK) for 1 h. Cell nuclei were stained with 0.25 µg/ml DAPI (4',6'-diamidine-2-phenylindole, Sigma) added to the secondary antibodies. mCherry-SOX2 expressing cells were only stained with DAPI. Slides were mounted with FluorSave Reagent (Calbiochem, Sigma-Aldrich Chemie GmbH Buchs, Switzerland) and images taken with a DMRE microscope (Leica Microsystems, Wetzlar, Germany) combined with an F-view camera (Soft Imaging System GmbH, Muenster, Germany). For mitochondria staining, cells were seeded on borosilicate 1.5-mm glass chambers (Lab-Tek II 8 well, Thermo Fischer Scientific) and co-stained with 12 nM mito-tracker green (Thermo Fischer Scientific #M7514) and 10 nM Hoechst dye (Thermo Fischer Scientific #H1398) for 30 minutes. Mitochondria were imaged with a spinning disk confocal microscope (Perkin Elmer, Waltham, MA, USA).

## Invasion assay

Boyden chambers (Cell Biolabs Inc, San Diego, CA, USA #CBA-100-C) were used according to manufacturer's instructions, with $5 \times 10^4$ cells for 24 h, except for BTB251 short-term cell culture ($7 \times 10^2$ cells). Invading cells were stained with DAPI and counted over five microscopic fields per well at 10× magnification. Experiments were performed 3 times in triplicate. Generation of necrotic cells for invasion assay in the presence of necrotic cells is based on Ahn *et al* (1). Necrotic cells were added to the autologous live cells at a ratio of 3:1.

## Zebrafish xenografts

Animal experiments and zebrafish husbandry were performed in accordance with the regulations of the veterinary office of the city of Basel (Kantonales Veterinäramt Basel Stadt, Basel, Switzerland). Cell Preparation: Preceding transplantation, LN319 cells were labeled with CellTracker™ CM-DiI (C7000, Life Technologies, Carlsbad, CA, USA) according to the manufacturer's instructions. In case of inducible *SOX2* overexpression, LN319 *TetON mCherry-SOX2* and the corresponding LN319 *TetON* control cells were first incubated with Doxycycline *in vitro* (1 µg/ml for 24 h) and labeled with CellTracker™ thereafter. Zebrafish Preparation: Wild-type zebrafish (TU, Tuebingen, "zfin.org") were maintained, collected and staged in E3 medium at 28.5°C according to standard procedures (40). For xenotransplantation experiments, zebrafish embryos were anesthetized in 0.4% tricaine

(Sigma) at 48-h postfertilization (hpf) and approximately 100 glioma cells microinjected into the vessel-free area of the yolk sack essentially as described (18). Cell transfer was verified by fluorescence microscopy after a recovery time of 1–2 h and fish harboring red cells shifted to 35°C thereafter. On assay day 5 (72-h post transplantation) animals were screened for persisting engraftment on a Zeiss Discovery V20 Stereo microscope supplied with an HXP120 fluorescent light source and further analyzed regarding tumor cell status on a Zeiss LSM 710 confocal microscope. Original image data were recorded in Zeiss Zen software and z-stack projections composed in Fiji (http://imagej.nih.gov) for optimal illustration. Experiments were performed in three independent biological replicates (n = 3) involving zebrafish embryos derived from several independent clutches.

## Pharmacology

PI3K/AKT/TOR signaling pathway inhibitors BYL-719, MK-2206, AKTi1/2 and rapamycin were all purchased from Selleckchem (Houston, TX, USA), dissolved and diluted according to manufacturer's instructions, and applied at the indicated concentrations for 48 h. For induction of mCherry-SOX2, p110α(WT), p110α(H1047R) and p110α(E545K) protein expression, cells were incubated with the indicated concentrations of doxycycline (D9891, Sigma, St-Louis, MO, USA) or standardly with 1 µg/ml for a minimum of 24 h.

## Chromatin immunoprecipitation

Chromatin immunoprecipitation was according to Carey *et al* (5). Chromatin immunoprecipitation of LN319 (sh*SOX2* vs. sh*scrambled*) was performed with either anti-SOX2 (Abcam #59776; Cambridge, UK) or IgG control (antibody Millipore, #12-170). Resulting DNA extract was subjected to quantitative real-time PCR of fragments containing the predicted SOX2-binding sites. Primers are listed in Table S2. Immunoprecipitation levels between LN319 sh*SOX2* (Santa Cruz Biotechnology sc-38408-V) and LN319 sh*scrambled* samples were normalized with Ct values from the IgG control. In each sample, immunoprecipitation with anti-SOX2 was calculated by subtraction of Ct value from control IgG immunoprecipitation.

## Cloning and site-directed mutagenesis

Genomic fragments of 3q26 gene promoters were amplified from HEK293 cell genomic DNA. PCR products were introduced into pGCL4.1 basic luciferase expression vector and sequenced. Site-directed mutagenesis was performed on cloned wild-type 3q26 promoters to destroy potential SOX2-binding sites. *MFN1* promoter was first produced as mutant and wild type was produced by reversing the mutation. Primers are listed in Table S2.

## Luciferase assay

HEK cells were transfected with the 3q26 gene promoter-luciferase reporter gene constructs using reagent JET PEI™

reagent (Polypus-transfection #101-01N). SOX2 was overexpressed by addition of an SOX2 expression vector (pMSCV-Flag-hSOX2, Addgene #2007). Luciferase activity was normalized with co-transfection of Renilla expression vector (pRL-null, Promega, Madison, WI, USA). Lysates were analyzed with the Dual Luciferase kit (Promega #E1980)

## Neuro-imaging

Volumetric imaging data were assessed for 65 GB patients from the most recent preoperative magnetic resonance imaging (MRI) from T2- and T1-weighted (native and contrast enhanced) as well as from Fluid Attenuated Inversion Recovery (FLAIR) images. In every instance, volumes for enhancing tumor, non-enhancing tumor, necrosis and total tumor were determined. These volumes were calculated using the ABC/2 method and expressed in mL. In addition, the tumor areas were calculated by multiplying the two largest axes, perpendicular to each other, determined from an axial contrast-enhanced T1-weighted image. This creates a two-dimensional plane through the tumor that is expressed in $mm^2$. Volume of recurrence was measured (mL) for tumors with documented recurrence.

## Statistics

Summary statistics of baseline demographics characteristics (age and gender) of the patient population are presented overall and separately for patients with and without a suitable MRI, together with summary statistics of the outcome variables corresponding to the primary endpoint (OS events, summaries of time to and surgery type). For continuous variables the number (n) of observations, median and interquartile range (IQR) are reported (Table S5).

The status of the genetic alteration is coded through a three-level categorical variable with the following genetic categories: (i) *SOX2* not amplified and *OPA1* not deleted, (ii) *SOX2* amplified and *OPA1* not deleted and (iii) *SOX2* not amplified and *OPA1* deleted. To assess the potential relationship between *SOX2* amplification or *OPA1* deletion and overall survival (OS) a Cox regression was fitted to the time of OS and the status of genomic aberration as factor of interest. The following variables are also included in the model to account for potential confounding: age and ratio of postoperative to preoperative tumor volume (log-transformed) as a measure of the extent of intervention.

To assess the relationship between alterations of *SOX2* and *OPA1* on parameters of tumor extension (including total volume, enhancing volume, necrosis volume, tumor area and recurrence volume) linear regression models were fitted to the genetic category as factor of interest. Age and the (log-transformed) ratio of postoperative to preoperative tumor volume are considered to account for potential confounding.

Independence between genomic alterations in *SOX2* and *OPA1* was assessed by Fisher exact test. With regards to

fish xenotransplant analyses, error bars represent the standard deviation (SD) of three independent biological replicates (n = 3), with a *T*-test score of $P \leq 0.05$ considered statistically significant (*).

## Mass spectrometry

Proteomics analysis of glioma biopsies was according to Dazert *et al* (8).

# RESULTS

## Regional imbalances at 3q26

*PIK3CA*, *MFN1*, *SOX2* and *OPA1* all map within 15 megabases at chromosome locus 3q26 (Figure 1A). In order to examine putative genetic imbalances at the gene level, we tested copy number variations of *PIK3CA*, *MFN1*, *SOX2* and *OPA1* in genomic DNAs from 129 glioma biopsies by quantitative PCR. Of the four genes, *SOX2* had the highest relative amplification frequency (26%) ranging from two- to eightfold absolute amplification, and *OPA1* the highest deletion frequency (19%) (Figure 1B). Similarly, data extraction of *SOX2* and *OPA1* CNV from the TCGA LGG and GB repositories revealed *ca* 10% amplification and deletion, respectively (Figure S3A). Quantitative comparison of *OPA1* CNV to those of *PTEN* and *CDKN2A* (frequently subject to hemizygous and homozygous deletion, respectively) suggest *OPA1* hemizygous rather than homozygous deletion. This was true for *IDH*-wild type ($IDH^{WT}$) glioma and *IDH*-mutant ($IDH^{mut}$) glioma (Figure S1B left), the prevailing marker used for glioma genetic classification (2). Moreover, we uncovered that *SOX2* genomic amplification (*SOX2*amp) and *OPA1* deletion (*OPA1*del) are mutually exclusive events ($P = 0.0044$, Figure S1B right). This raised the question whether both events lead to a common oncogenic phenotype. Consistent with an oncogenic relevance of *SOX2*amp and *OPA1*del, a comparison of glioma biopsies of various histology to non-tumor brain tissue on the *Rembrandt* database (>400 glioma) showed higher *SOX2* mRNA levels and lower *OPA1* mRNA levels in GB and in LGG (astrocytoma and oligodendroglioma). Moreover, both variations were in addition significantly associated with shorter survival time (Figure S3B). We then tested the relative expression levels of SOX2 and OPA1 proteins in six representative biopsies by mass spectrometry. Regardless of *IDH* mutation, *SOX2*amp or *OPA1*del statuses, SOX2 protein levels were always considerably higher and OPA1 reduced in glioma tissue sample compared to non-neoplastic white matter control tissues (Figure 1C). The discrepancy between *SOX2* and *OPA1* copy number variations and protein levels may be attributed to transcriptional and/or posttranslational regulation. Nevertheless, genomic, transcriptomic and protein data all point to SOX2 gain-of-function and OPA1 loss-of-function in glioma. Taken all results together, we accumulated arguments on the oncogenic relevance of *SOX2* gain and *OPA1* loss.

## Mimicking 3q26 gene imbalances in glioma line LN319

To perform SOX2 gain and OPA1 loss functional investigations in vitro, we initially screened a panel of glioma-derived cell lines for overt abnormalities in 3q26 gene expression. Out of eight tested cell lines, only two, LN319 and U373, showed robust SOX2 protein expression (Figure S1C, top). Of these, LN319 had nuclear localization of SOX2 (Figure S1C) predicting transcriptionally active SOX2, no aneuploidy at *SOX2* and *OPA1* genes and no *PIK3CA* coding sequence mutation, while U373 had mostly cytosolic SOX2 (Figure S1C), likely to be transcriptionally inactive, and triploidy at 3q26 (37). For these reasons, we focused our investigations on LN319 as primary study tool. We mimicked SOX2 overexpression in LN319 cells with a stably integrated and inducible mCherry-*SOX2* fusion construct that showed a preferential nuclear localization upon induction (Figure 2A). Conversely, we inactivated *OPA1* through stable knockdown with shRNA, with mitochondria shortening as resulting phenotype (Figure 2B). Both *SOX2* overexpression and *OPA1* inactivation led to higher relative cell invasion rates (Figure 2A,B, right). In both cases, increased invasion rates were accompanied by reduced proliferation rates (Figure S4). Knock-down of *OPA1* in U373 cells led to a slight but nonsignificant invasion increase, consistent with the predicted low SOX2 transcriptional activity in parental U373 (Figure S1C). Among short-term cell cultures grown *ex vivo* from resected human gliomas, only one, BTB251, showed no CNV at 3q26 genes, could be stably transfected for OPA1 knockdown and propagated for assessment of invasion potential. Invasion rate of BTB251 was increased when OPA1 was knocked-down, although not to a degree of significance (Figure S1D).

We then referred to xenotransplant experiments to examine the functional significance of our findings under *in vivo* conditions. Either LN319 *OPA1* knock-down or LN319 *SOX2* overexpression cells were microinjected into the yolk sack of zebrafish embryos and the propagation and spreading of the injected specimen analyzed over time (Figure 3A,B, respectively). We found that, in comparison to respective controls, both *OPA1* los*s* and *SOX2* gain increased the propensity of cells to leave the site of injection, to spread and invade the yolk sack, and—in a fair number of cases—to even disseminate into distal zones of the fish body, *that is,* the caudal hematopoietic tissue (CHT) of the tail fin. It is noteworthy that these effects were more pronounced in *OPA1* loss than in *SOX2 gain* cells, which may reflect the intrinsically high endogenous SOX2 level of the LN319 strain background. In any case though, we provide cumulative experimental evidence to suggest that *OPA1* loss and *SOX2* gain promote invasiveness of glioma cells *in vitro* and *in vivo*.
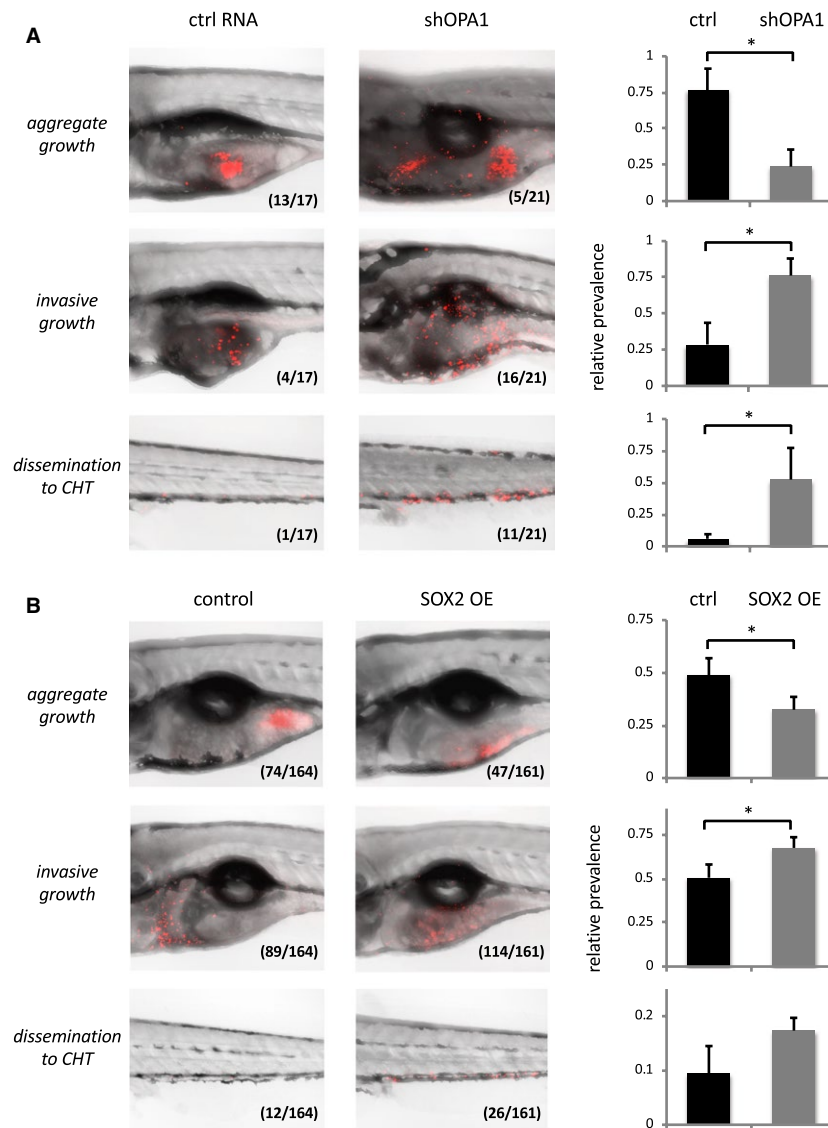
**Figure 3.** **A.** *OPA1* knock-down increases invasiveness of LN319 cells *in vivo*. Left: Confocal pictures of zebrafish embryos effectively xenotransplanted with LN319 control cells (shRNA non-coding, left) or LN319 *shOPA1* knock-down cells (right). LN319 cells (Cell Tracker, red) either established stable cell masses near the site of injection (aggregate growth, top), dispersed throughout the yolk sack (invasive growth, center) or disseminated to the caudal hematopoietic tissue (CHT) of the tail fin (bottom). Inlays indicate absolute animal numbers per condition. Right: Relative quantification of experimental outcomes documenting aggravated invasiveness and dissemination of *OPA1* knock-down vs. respective control cells. **B.** *SOX2* overexpression (OE) increases invasiveness of LN319 cells *in vivo*. Experimental setup as above, except that *TetON* (control, left) and *TetON mCherry-SOX2* (*SOX2* OE, right) cells had been pretreated with doxycycline (1 µg/ml for 24 h) to selectively induce SOX2 protein formation prior to transplantation. Right: Assay quantification verifying increased invasiveness and dissemination to CHT (by trend) also for *SOX2* OE cells when compared to equally treated controls. Significance cut-off-: *$P < 0.05$.

## PI3K/AKT activates SOX2

Overexpression of PIK3CA (alias p110α, the catalytic subunit of PI3 kinase) in LN319 increases phosphorylation of AKT, which leads to an activation of the mammalian target of Rapamycin complex 1 (mTORC1) and further downstream effectors such as ribosomal protein RPS6. More importantly, overexpression of PIK3CA coincided with elevated steady-state levels of also SOX2, thus underscoring a functional relevance of the PI3K/AKT signaling axis for SOX2 expression (Figure 4A, left). The latter effect was even more pronounced when constitutively active alleles of PIK3CA (H1047R or E545K) were expressed (Figure 4A, right). Based on these findings and the previously described role of PIK3CA on posttranslational SOX2 activation in breast cancer (30), we went on to selectively inactivate PI3K, AKT or mTORC1 with respective inhibitory reagents in LN319 glioma cells (see Figure 4E for schematic illustration of compounds and
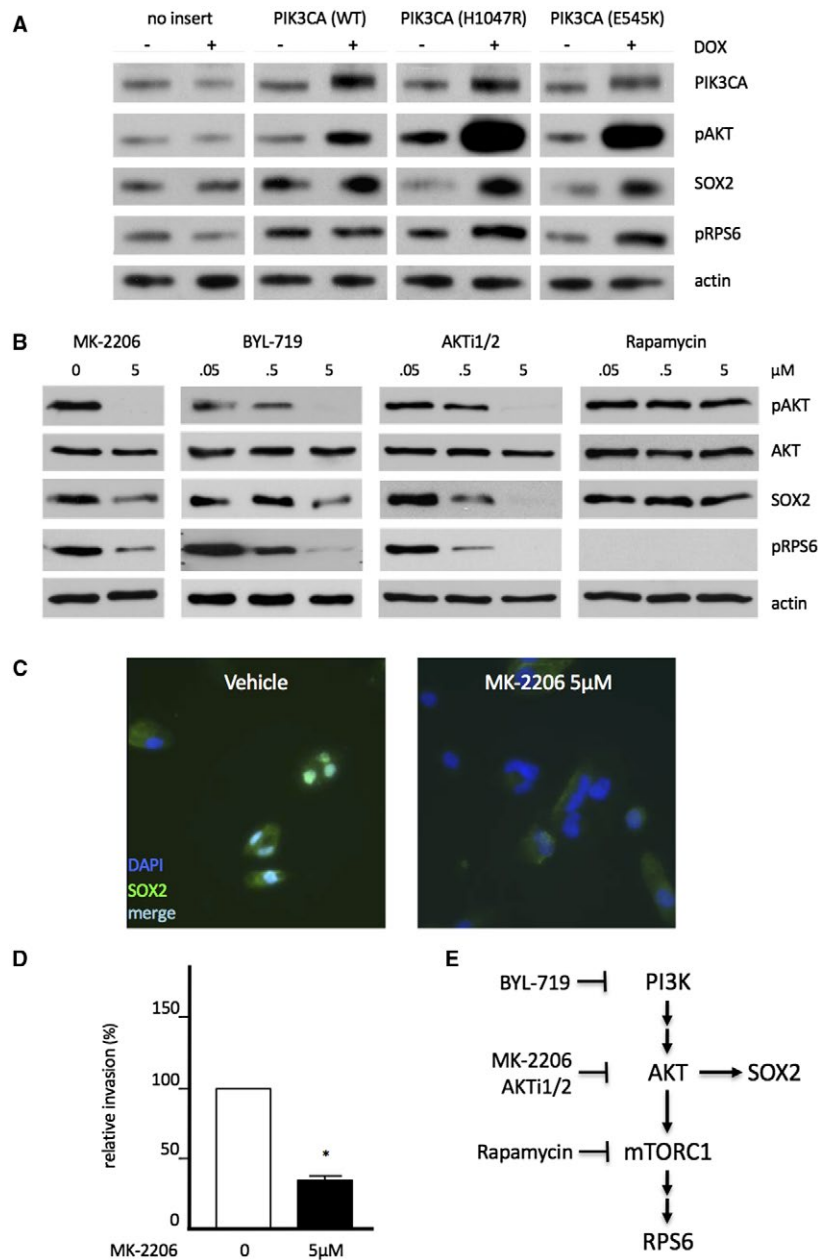
**Figure 4.** Modulation of SOX2 protein stability by canonical PI3K/AKT signaling. **A.** Increased PI3K activity fosters SOX2 protein expression in LN319 cells. Cell were stably transfected with Doxycycline-inducible variants of *PIK3CA* encoding the catalytic subunit of PI3 kinase p110. From left to right: no insert (control), *PIK3CA* wild type, and the constitutively active mutant alleles H1047R or E545K. Note elevated SOX2 protein expression in response to aggravated PI3K activity, as indicated by increased pAKT (Ser473) and pS6 (Ser235,236) signatures. Actin staining is shown for loading control. **B.** Effects of 48 h-exposure to PI3K/AKT/TOR pathway inhibitors on SOX2 protein levels as assessed by Western blot. SOX2 expression is strongly impaired by pan PI3K-inhibitor (BYL-719) and AKT-inhibitors (AKTi1/2, MK-2206), but not by further downstream inhibitor rapamycin (anti mTORC1). **C.** Fluorescence microcopy to document nucleo-cytoplasmatic displacement and reduction of SOX2 protein expression by PI3K inhibitor MK-2206. **D.** Impaired invasiveness of MK-2206-treated, SOX2-depleted LN319 cells as assayed by Boyden chamber experiments. **E.** Schematic illustration of SOX2 protein expression and turnover in dependence of PI3K/AKT signaling.

targets). Indeed, suppression of PI3 kinase activity by BYL-719 or of its downstream factor AKT by either MK-2206 or AKTi1/2, as all indicated by drug-induced loss of pSer437 AKT signal, led to decreased SOX2 levels. In contrast, inhibition of even further downstream mTORC1 by rapamycin, resulted in strong reduction of pRPS6, but did not affect SOX2 protein levels (Figure 4B). Accordingly, PI3K/AKT signaling influenced SOX2 protein turnover independently of
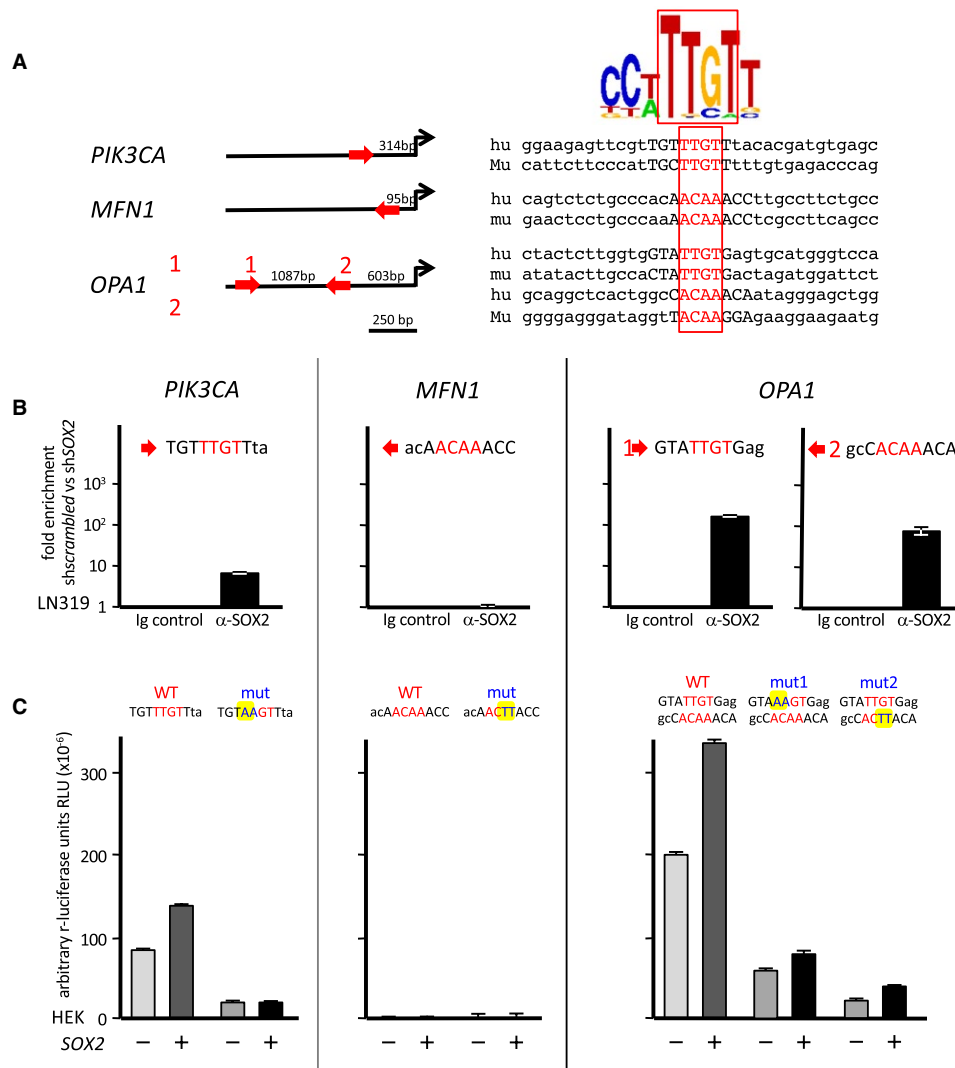
**Figure 5.** SOX2 *trans*-activates 3q26 genes *PIK3CA* and *OPA1*. **A.** Theoretical SOX2-binding sequences found upstream of *PIK3CA*, *MFN1* and *OPA1* transcription initiation sites. **B.** ChIP of *PIK3CA*, *MFN1* and *OPA1* promoter regions containing the potential SOX2-binding sites (LN319 cells). **C.** Luciferase assays of *PIK3CA*, *MFN1* and *OPA1* promoter regions containing the potential SOX2-binding sites (HEK293 cells). Co-transfection of SOX2 expressing vector and comparison between wild-type and mutated sites.

mTORC1 (Figure 4B,E). What is more, AKT inhibitor MK-2206 effectively displaced SOX2 from the nucleus and largely depleted cells of SOX2 (Figure 4C), which correlates once again with largely decreased relative invasion rates (Figure 4D). From these observations, we concluded that PI3K influences the localization and stability of SOX2 protein, thus fostering its activity in glioma cells. These findings further underscore a functional connectivity between products of the 3q26 segment and emphasize PI3K/AKT pathway inhibitors as potential drug candidates in glioma.

## SOX2 trans-activates PIK3CA, OPA1, but not MFN1

Given that SOX2 is a transcriptional modulator, we tested whether 3q26 genes could be regulated by SOX2, which

was supported by the presence of potential SOX2-binding sites upstream of *PIK3CA*, *MFN1* and *OPA1* transcription initiation sites (Figure 5A). Physical binding of SOX2 to genomic fragments containing the predicted SOX2-binding sites was tested by chromatin immunoprecipitation (ChIP) first. We observed significantly higher immunoprecipitation in the presence of anti-SOX2 compared to isotype control antibodies for the *PIK3CA* site and for both *OPA1* sites (Figure 5B). However, no binding was seen for the *MFN1* fragment. To test the potential activation of transcription by SOX2 on 3q26 gene promoters, we constructed plasmids in which the luciferase reporter gene was under the control of *PIK3CA*, *MFN1* and *OPA1* promoter fragments containing the potential SOX2-binding sites. In parallel, we disrupted the predicted potential SOX2-binding sites by site-directed
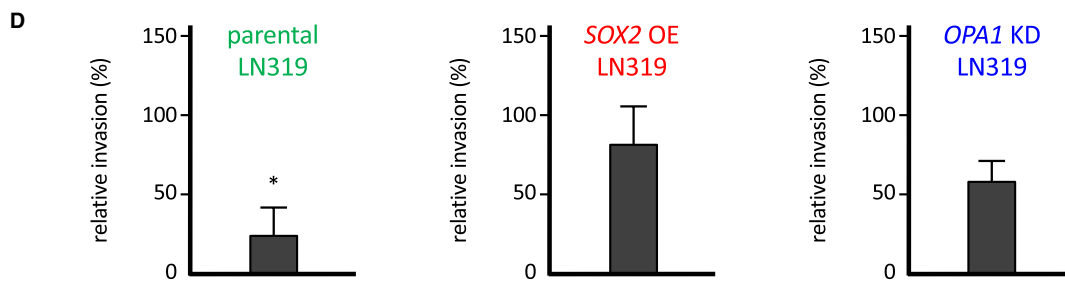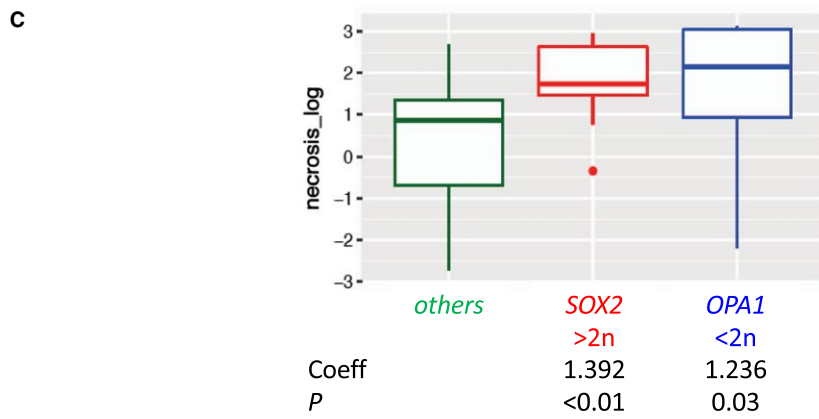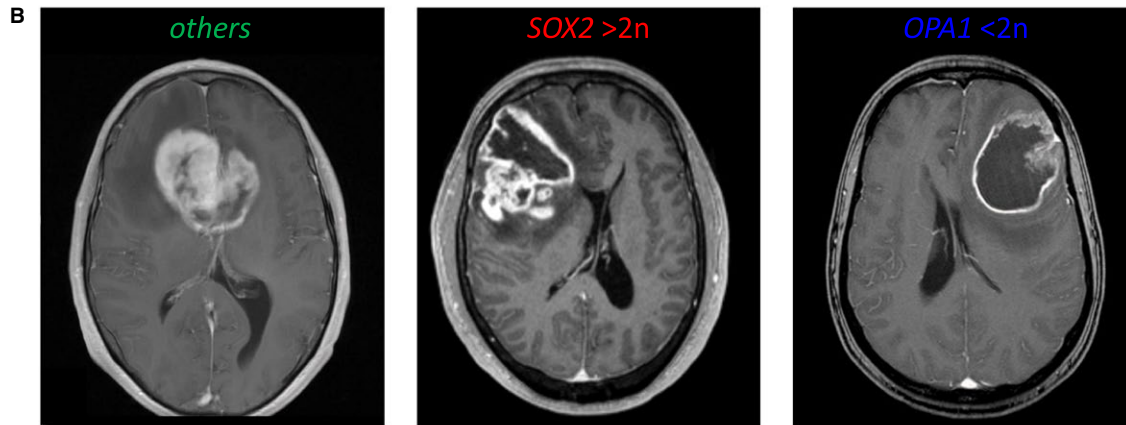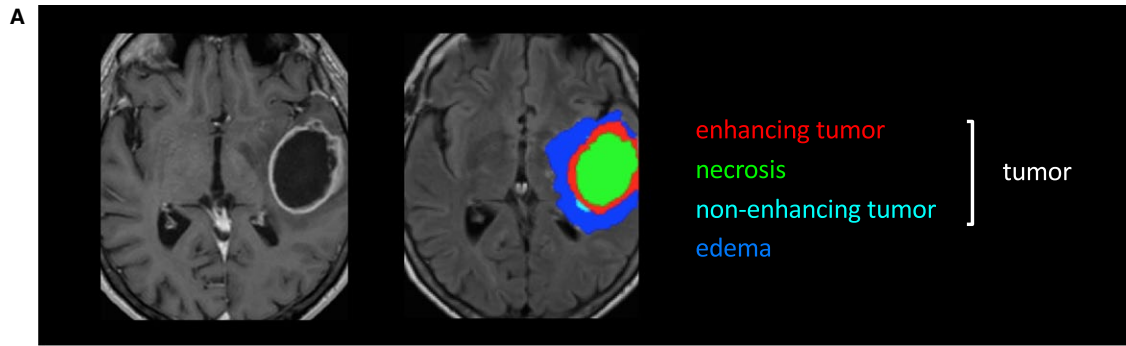
**Figure 6.** *SOX2* amplification and *OPA1* deletion are associated with larger necrotic volumes in the glioma mass. **A.** Neuroimaging (left) and color modelization (right) of the tumor compartments of the same glioma. **B.** Neuroimaging of representative glioma cases with neither *SOX2* amplification nor *OPA1* deletion (left) with *SOX2* amplification (center) and *OPA1* deletion (right). **C.** Boxplots visualizing the distribution of the log-transformed volume of necrotic compartment of gliomas across different statuses of *SOX2* and *OPA1*. The boxes display the median and the interquartile range. Coefficients estimates for a linear model with log-transformed necrosis volume and adjusted for age and ratio of postoperative to preoperative volume are shown below the boxplots. **D.** Comparative invasion kinetics of LN319 cells in the presence of autologous necrotic LN319 cells. Parental LN319 (left), LN319 overexpressing *cherry-SOX2* under the control of 30 ng/ml doxycycline (middle) and L319 with *OPA1* knocked down by shRNA (right). Invasiveness in absence of necrotic cells was set to 100% (reference score). Significance cutoff: $*P < 0.05$.

mutagenesis. Constructs were transfected into human embryonic kidney HEK293 cells, in the presence or absence of a plasmid expressing additional SOX2. Figure 5C shows an active *PIK3CA* promoter that responded to additional SOX2, while introduction of mutations into the potential SOX2-binding site abrogated promoter activity and response to SOX2 (left). Reflecting the presence of even two binding sites, the *OPA1* promoter showed an even higher activity and response to SOX2 than the aforementioned *PIK3CA*. Consistently, introduction of mutations in either site partly diminished promoter activity and responsiveness to SOX2 (right). Instead, we found no experimental evidence for a SOX2 dependent promoter regulation of *MFN1* (middle). Altogether, ChIP and luciferase assays consistently showed that *PIK3CA* and especially *OPA1* are target genes of SOX2, whereas *MFN1* is not.

## Alterations of SOX2 and OPA1 impact neuroimaging parameters of tumor extension

We wanted to see if there is an association between tumor size (measured by neuroimaging) and *SOX2*amp or *OPA1*del on glioma invasion (Figure S5 and Table S6). Towards this goal, we implemented linear models linking the genomic alteration to the following parameters: non-enhancing volume (lower grade tumor compartment), enhancing volume (malignant tumor component), necrosis (within tumor core, hallmark of GB), total volume (enhancing + non-enhancing + necrosis) and preoperative maximal tumor area on the axial plane as parameters. An illustrated example is given in Figure 6A. The postoperative parameter was recurrence volume. To account for confounding, we also included age at surgery, and the log-transformed ratio of postoperative to preoperative volume in the model. As *SOX2*amp and *OPA1*del are mutually exclusive events, we considered them as distinct glioma genetic entities to be analyzed for neuroimaging. From the linear model linking the genetic alteration with the log-transformed necrosis volume, where we also included age at surgery and the log-transformed ratio of postoperative to preoperative volume to account for confounding, we saw that both *SOX2*amp and *OPA1*del are associated with the necrosis tumor volume (Table S7, Figure 6A,B). In particular, we observed that the presence of *SOX2*amp was associated with a fourfold increase, while *OPA1*del, with a 3.4-fold increase in the tumor necrosis volume with respect to the case with neither *SOX2*amp nor *OPA1*del (Figure 6B,C). In addition, higher tumor area extension tended to be associated with both genetic markers (Figure S8 and Table S9). To mimic a possible role of necrotic tissue on tumor cell invasion, we performed invasion assays of parental LN319 and LN319 cells engineered to overexpress SOX2 or inactivate OPA1 in the presence of necrotic autologous cells. Addition of necrotic cells impaired parental LN319 invasiveness (Figure 6D, left). However, relative to parental LN319, both SOX2-overexpressing and OPA1-inactivating LN319 strains had higher invasion rates (3.4- and 2.3-fold, respectively) in the presence of necrotic cells (Figure 6D, middle and right), suggesting that that an overall invasion-inhibitory effect of necrotic cells is largely overruled by *SOX2* amplification or *OPA1* loss in LN319 cells.

Based on our observations that *SOX2* gain or *OPA1* loss both induce glioma cell invasion *in vitro, in vivo* in xenotransplant studies, and are both associated with larger necrotic area revealed by neuroimaging of human glioma, we postulate a functional connectivity between necrosis and invasion in glioblastoma.

# DISCUSSION

## SOX2 and OPA1 status in glioma

Approximately 10% of LGG and GB patient samples deposited in the TCGA database show *SOX2* amplification or *OPA1* deletion (Figure S3A), with no further reported investigation. Preferential *SOX2*amp and *OPA1*del occur independently of the *IDH* status, the major genetic determinant in diffuse gliomas. This indicates that *SOX2*amp and *OPA1*del promote cell invasiveness regardless of the glioma developmental pathway. Two hypotheses may account for the mutual exclusion between *SOX2*amp and *OPA1*del. First, mutual exclusivity can be an indicator for a commonly targeted phenotype, like invasion in this case. Alternatively, as *SOX2* and *OPA1* cluster within only 15 megabases at 3q26, amplification or deletion of one is likely to involve the neighboring gene too, which reduces the likelihood of concomitant *SOX2*amp and *OPA1*del events. This hypothesis is supported by the analysis of the TCGA database, where individual samples with *OPA1* amplification show common amplification of *SOX2*, *PIK3CA* and *MFN1*, suggesting that *SOX2* amplification events may extend to *OPA1* gene (Figure S3A, red top bands). While we observed a mutual exclusion of *SOX2* gene amplification and *OPA1* deletion in our patient collection, we noticed that at the protein level, SOX2 gain and OPA1 loss are concomitant in distinct glioma
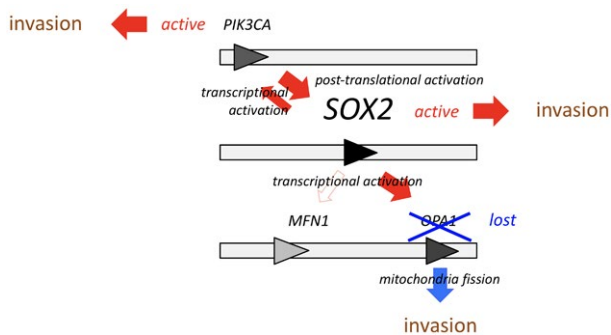
**Figure 7.** 3q26 gene products modulate glioma cell invasion in various entangled ways. SOX2 balances glioma cell invasion through intrinsically antagonistic mechanisms: While PI3K/AKT/mTOR (41) and PI3K/AKT-SOX2 loops promote glioma invasion (9,20), SOX2 *trans*-activates *OPA1*, which results in an effective inhibition of invasion. OPA1 knock-down mutations resolve this functional antagonism and lead to an effective deregulation of glioma cell invasion.

genotypes, considering *IDH* mutation, *SOX2*amp or *OPA1*del statuses. This concomitance suggests that optimization of invasion requires further mechanisms downstream of gene copy variation, possible epigenetic and posttranslational regulation events.

## Interplay between 3q26 genes

Consistent with previous data on breast cancer cells (30), we found that SOX2 was displaced from nucleus to cytosol in response to inhibition of the PI3K/AKT pathway. Maintaining SOX2 activation by PI3K/AKT pathway activity provided a first molecular link between the 3q26 gene products PIK3CA and SOX2. Of note, mTOR, a downstream target of PI3K/AKT signaling, was previously identified as a regulator of glioma cell invasion and proposed as target for controlling cell invasion (6). However, we found that PI3K/AKT directly regulates SOX2 activity in ways that do not (evidently) involve mTORC1. Furthermore, SOX2 *trans*-activates *PIK3CA* as part of a positive feedback loop to further maintain cell invasion. Interestingly, SOX2 has been previously shown to activate the Notch pathway to promote glioma cell invasion (32,43). Proteins involved in mitochondria fusion (OPA1 and MFN1) or fission (DRP1) have been shown to positively (DRP1) and negatively (OPA1 and MFN1) regulate cell motility (10,11). mTOR, an activator of glioma invasion, has also been shown to induce mitochondria fission through DRP1 recruitment (6,24). Thus, AKT seems to drive two distinct mechanisms of glioma cell invasion activation, an mTOR-dependent, presumably through DRP1 activation and an mTOR-independent mechanism through SOX2. However, the concomitant *trans*-activation of *OPA1* and *PIK3CA* results in a conflicting situation between the pro-invasive PI3K/AKT-mTOR-DRP1 and PI3K/AKT-SOX2 pathways, and invasion suppression by the PI3K/AKT-SOX2-OPA1 axis.

Loss of OPA1 function—otherwise activated by SOX2 as shown here by Chip and Luciferase reporter assay—would therefore be a response to optimize invasion capacity from PI3K/AKT and SOX2 pathways (Figure 7).

## Necrosis and invasion

The mutual exclusion between *SOX2*amp and *OPA1*del suggested that both glioma genetic entities could result in a similar phenotype. We used this assumption as a rationale for stratifying the alterations in SOX2 and OPA1 as a categorical variable with three levels in order to assess the association between *SOX2*/*OPA1* status and tumor size parameters. Indeed, considering *SOX2* gain *vs.* no *SOX2* gain, no *SOX2* gain would have also included *OPA1* loss and conversely, *OPA1* loss *vs.* no *OPA1* loss, no *OPA1* loss would have included *SOX2* gain. Thus, in both cases, *SOX2* gain and *OPA1* loss would mask each other, potentially reducing the difference seen in the phenotype associated to each category. In a homogenous population of GB, tumor area tended to be associated with *SOX2*amp or *OPA1*del ($P < 0.15$). For the necrotic compartment volume, we observed a stronger association and significance in both cases ($P = 0.01$ and $P = 0.03$, respectively). This is consistent with recent results showing that the vicinity of necrotic tissue induces chemokine IL-8 production by GB cells resulting in enhanced invasion in CRT-MG cells (1). In LN319 cells, *relative* to parental strain, we observed that the presence of autologous necrotic cells increased invasion under conditions of either SOX2 gain or OPA1 loss. This suggests that SOX2 gain or OPA1 loss may play a role in this process, either in the necrotic cells, or in the invading cells, the underlying mechanism remaining to be investigated.

This could imply that the volume of the necrotic compartment could indeed represent an indirect biomarker to assess invasion. Nevertheless, due to the limited sample size, no strong relationship could be established between *SOX2*amp or *OPA1*del with overall survival (Table S9). The non-enhancing compartment visualized by MRI may also include vasogenic edema of inflammatory origin which may lead to an overestimation of the volume (illustrated in Figure 6A). The infiltration zone, representing a gradient of progressive dilution of sparse invading tumor cells, cannot be accurately determined. Based on these observations, the necrotic volume compartment of the tumor turned out to be the most accurate value and is therefore a suitable surrogate marker for assessing invasion.

## Pathways to be targeted to control invasion

Several pathways have been identified to induce cell motility and have been postulated as potential targets for controlling glioma cell invasion, such as, for example, mTOR (6). The PI3K/AKT/SOX2 axis described here imposes a natural limitation to any such efforts, as PI3K and SOX2 interact essentially independent of mTOR (see Figure 4B/E). Further upstream PI3KCA or AKT, both at the crossroads of mTOR-dependent and SOX2-driven branches of invasion

modulation, may thus provide more suitable targets to restrict glioma cell invasion for clinical purposes. Also, mitochondria fusion protein OPA1 inactivation could potentially be counteracted by inactivation of, for example, mitochondria fission protein DRP1. Regarding cause-and-effect relationship, whether SOX2 gain or OPA1 loss either trigger tumor cell necrosis itself or sensitize tumor cells for paracrine responses to induce necrosis remains to be resolved.

Taken together, we unraveled a functional interplay of 3q26 gene products in the regulation of glioma cell invasion. OPA1 loss and SOX2 gain mutations in particular stimulate glioma cell invasiveness *in vitro* and *in vivo,* and coincide with elevated necrotic volume scoring in neuroimages of patients. Our molecular findings thus meet a phenotypic disease manifestation that may influence disease scoring in the future. This strengthens the need for combinatorial therapies that would target multiple pathways and pathway branches for controlling invasive tumor expansion.

## AUTHOR'S CONTRIBUTIONS

**Conception and design:** JL Boulay, L Mariani, S Frank, T Schaefer

**Development of methodology:** MF Ritz, C Tostado, A Ramadoss

**Acquisition of data (provided animals, acquired and managed patients, provided facilities, etc.):** JL Boulay, L Mariani, MF Ritz, C Lengerke, H Neddersen, S Falbo, C Stippich, A Bink, P Demougin, P Jenö, S Moes, C Tostado, L Tintignac, Christoph Schürch, Joëlle Müller, Jonas Schärer, S Leu, A Ramadoss, T Schaefer

**Analysis and interpretation of data (eg, statistical analysis, biostatistics, computational analysis):** JL Boulay, L Mariani, MF Ritz, H Bucher, A Bink, P Demougin, P Jenö, S Moes, G Moffa, L Tintignac, S Leu, A Ramadoss, T Schaefer

**Writing, review, and/or revision of the manuscript:** JL Boulay, L Mariani, S Frank, C Lengerke, A Bink, P Jenö, G Moffa, S Leu , T Schaefer

**Administrative, technical, or material support (ie, reporting or organizing data, constructing databases):** C Tostado, T Schaefer, S Leu,

## CONFLICT OF INTEREST

No potential conflicts of interest were disclosed

## ACKNOWLEDGMENTS

## REFERENCES

1. Ahn SH, Park H, Ahn YH, Kim S, Cho MS, Kang JL, Choi YH (2016) Necrotic cells influence migration and invasion of glioblastoma via NF-κB/AP-1-mediated IL-8 regulation. *Sci Rep* **6**:24552.
2. Alonso MM, Diez-Valle R, Manterola L, Rubio A, Liu D, Cortes-Santiago N, *et al* (2011) Genetic and epigenetic modifications of Sox2 contribute to the invasive phenotype of malignant gliomas. *PLoS One* **6**:e26740.
3. Ben-Porath I, Thomson MW, Carey VJ, Ge R, Bell GW, Regev A, Weinberg RA (2008) An embryonic stem cell-like gene expression signature in poorly differentiated aggressive human tumors. *Nat Genet* **40**:499–507.
4. Campello S, Lacalle RA, Bettella M, Mañes S, Scorrano L, Viola A (2006) Orchestration of lymphocyte chemotaxis by mitochondrial dynamics. *J Exp Med* **203**:2879–2886.
5. Carey KT, Tan KH, Ng J, Liddicoat DR, Godfrey DI, Cole TJ (2013) Nfil3 is a glucocorticoid-regulated gene required for glucocorticoid-induced apoptosis in male murine T cells. *Endocrinology* **154**:1540–1552.
6. Chandrika G, Natesh K, Ranade D, Chugh A, Shastry P (2016) Suppression of the invasive potential of Glioblastoma cells by mTOR inhibitors involves modulation of NFκB and PKC-α signaling. *Sci Rep* **6**:22455.
7. Cuddapah VA, Robel S, Watkins S, Sontheimer H (2014) A neurocentric perspective on glioma invasion. *Nat Rev Neurosci* **15**:455–465.
8. Dazert E, Colombi M, Boldanova T, Moes S, Adametz D, Quagliata L, *et al* (2016) Quantitative proteomics and phosphoproteomics on serial tumor biopsies from a sorafenib-treated HCC patient. *Proc Natl Acad Sci U S A* **113**:1381–1386.
9. Delettre C, Lenaers G, Griffoin JM, Gigarel N, Lorenzo C, Belenguer P, *et al* (2000) Nuclear gene OPA1, encoding a mitochondrial dynamin-related protein, is mutated in dominant optic atrophy. *Nat Genet* **26**:207–210.
10. Desai SP, Bhatia SN, Toner M, Irimia D (2013) Mitochondrial localization and the persistent migration of epithelial cancer cells. *Biophys J* **104**:2077–2088.
11. Ferreira-da-Silva A, Valacca C, Rios E, Pópulo H, Soares P, Sobrinho-Simões M, *et al* (2015) Mitochondrial dynamics protein Drp1 is overexpressed in oncocytic thyroid tumors and regulates cancer cell migration. *PLoS One* **10**:e0122308.
12. Friedl P, Alexander S (2011) Cancer invasion and the microenvironment: plasticity and reciprocity. *Cell* **147**:992–1009.
13. Gangemi RM, Griffero F, Marubbi D, Perera M, Capra MC, Malatesta P, *et al* (2009) SOX2 silencing in glioblastoma tumor-initiating cells causes stop of proliferation and loss of tumorigenicity. *Stem Cells* **27**:40–48.
14. Gao H, Teng C, Huang W, Peng J, Wang C (2015) SOX2 promotes the epithelial to mesenchymal transition of esophageal squamous cells by modulating slug expression through the activation of STAT3/HIF-α signaling. *Int J Mol Sci* **16**:21643–21657.
15. Hammoud MA, Sawaya R, Shi W, Thall PF, Leeds NE (1996) Prognostic significance of preoperative MRI scans in glioblastoma multiforme. *J Neurooncol* **27**:65–73.

16. Ikushima H, Todo T, Ino Y, Takahashi M, Miyazawa K, Miyazono K (2009) Autocrine TGF-beta signaling maintains tumorigenicity of glioma-initiating cells through Sry-related HMG-box factors. *Cell Stem Cell* **5**:504–514.

17. Ishii N, Maier D, Merlo A, Tada M, Sawamura Y, Diserens AC, Van Meir EG (1999) Frequent co-alterations of TP53, p16/CDKN2A, p14ARF, PTEN tumor suppressor genes in human glioma cell lines. *Brain Pathol* **9**:469–479.

18. Konantz M, Balci TB, Hartwig UF, Dellaire G, André MC, Berman JN, Lengerke C (2012) Zebrafish xenografts as a tool for *in vivo* studies on human cancer. *Ann N Y Acad Sci* **1266**:124–137.

19. Kondziolka D, Lunsford LD, Martinez AJ (1993) Unreliability of contemporary neurodiagnostic imaging in evaluating suspected adult supratentorial (low-grade) astrocytoma. *J Neurosurg* **79**:533–536.

20. Kubiatowski T, Jang T, Lachyankar MB, Salmonsen R, Nabi RR, Quesenberry PJ, et al (2001) Association of increased phosphatidylinositol 3-kinase signaling with increased invasiveness and gelatinase activity in malignant gliomas. *J Neurosurg* **95**:480–488.

21. Li X, Xu Y, Chen Y, Chen S, Jia X, Sun T, et al (2013) SOX2 promotes tumor metastasis by stimulating epithelial-to-mesenchymal transition via regulation of WNT/β-catenin signal network. *Cancer Lett* **336**:379–389.

22. Louis DN, Perry A, Reifenberger G, von Deimling A, Figarella-Branger D, Cavenee WK, et al (2016) The 2016 World Health Organization Classification of Tumors of the Central Nervous System: a summary. *Acta Neuropathol* **131**:803–820.

23. Luo W, Li S, Peng B, Ye Y, Deng X, Yao K (2013) Embryonic stem cells markers SOX2, OCT4 and Nanog expression and their correlations with epithelial-mesenchymal transition in nasopharyngeal carcinoma. *PLoS One* **8**:e56324.

24. Morita M, Prudent J, Basu K, Goyon V, Katsumura S, Hulea L, et al (2017) mTOR Controls Mitochondrial Dynamics and Cell Survival via MTFP1. *Mol Cell* **67**:922–35.e5.

25. Network CGAR (2008) Comprehensive genomic characterization defines human glioblastoma genes and core pathways. *Nature* **455**:1061–1068.

26. Park GB, Kim D (2017) TLR5/7-mediated PI3K activation triggers epithelial-mesenchymal transition of ovarian cancer cells through WAVE3-dependent mesothelin or OCT4/SOX2 expression. *Oncol Rep* **38**:3167–3176.

27. Paw I, Carpenter RC, Watabe K, Debinski W, Lo HW (2015) Mechanisms regulating glioma invasion. *Cancer Lett* **362**:1–7.

28. Raza SM, Lang FF, Aggarwal BB, Fuller GN, Wildrick DM, Sawaya R (2002) Necrosis and glioblastoma: a friend or a foe? A review and a hypothesis. *Neurosurgery* **51**:2–12; discussion-3.

29. Samuels Y, Wang Z, Bardelli A, Silliman N, Ptak J, Szabo S, et al (2004) High frequency of mutations of the PIK3CA gene in human cancers. *Science* **304**:554.

30. Schaefer T, Wang H, Mir P, Konantz M, Pereboom TC, Paczulla AM, et al (2015) Molecular and functional interactions between AKT and SOX2 in breast carcinoma. *Oncotarget* **6**:43540–43556.

31. Scherer HJ (1940) A critical review: the pathology of cerebral gliomas. *J Neurol Psychiatry* **3**:147–177.

32. Sivasankaran B, Degen M, Ghaffari A, Hegi ME, Hamou MF, Ionescu MC, et al (2009) Tenascin-C is a novel RBPJkappa-induced target gene for Notch signaling in gliomas. *Cancer Res* **69**:458–465.

33. Song Z, Ghochani M, McCaffery JM, Frey TG, Chan DC (2009) Mitofusins and OPA1 mediate sequential steps in mitochondrial membrane fusion. *Mol Biol Cell* **20**:3525–3532.

34. Stemke-Hale K, Gonzalez-Angulo AM, Lluch A, Neve RM, Kuo WL, Davies M, et al (2008) An integrative genomic and proteomic analysis of PIK3CA, PTEN, and AKT mutations in breast cancer. *Cancer Res* **68**:6084–6091.

35. Suvà ML, Rheinbay E, Gillespie SM, Patel AP, Wakimoto H, Rabkin SD, et al (2014) Reconstructing and reprogramming the tumor-propagating potential of glioblastoma stem-like cells. *Cell* **157**:580–594.

36. Tan EJ, Olsson AK, Moustakas A (2015) Reprogramming during epithelial to mesenchymal transition under the control of TGFβ. *Cell Adh Migr* **9**:233–246.

37. Torsvik A, Stieber D, Enger P, Golebiewska A, Molven A, Svendsen A, et al (2014) U-251 revisited: genetic drift and phenotypic consequences of long-term cultures of glioblastoma cells. *Cancer Med* **3**:812–824.

38. Wangaryattawanich P, Hatami M, Wang J, Thomas G, Flanders A, Kirby J, et al (2015) Multicenter imaging outcomes study of The Cancer Genome Atlas glioblastoma patient cohort: imaging predictors of overall and progression-free survival. *Neuro Oncol* **17**:1525–1537.

39. Wen PY, Macdonald DR, Reardon DA, Cloughesy TF, Sorensen AG, Galanis E, et al (2010) Updated response assessment criteria for high-grade gliomas: response assessment in neuro-oncology working group. *J Clin Oncol* **28**:1963–1972.

40. Westfield M (2000) The Zebrafish Book. A Guide for the Laboratory Use of Zebrafish (danio rerio), 4th edn. University of Oregon Press: Eugene.

41. Wick W, Platten M, Weller M (2001) Glioma cell invasion: regulation of metalloproteinase activity by TGF-beta. *J Neurooncol* **53**:177–185.

42. Yang N, Hui L, Wang Y, Yang H, Jiang X (2014) Overexpression of SOX2 promotes migration, invasion, and epithelial-mesenchymal transition through the Wnt/β-catenin pathway in laryngeal cancer Hep-2 cells. *Tumour Biol* **35**:7965–7973.

43. Ying M, Wang S, Sang Y, Sun P, Lal B, Goodwin CR, et al (2011) Regulation of glioblastoma stem cells by retinoic acid: role for Notch pathway inhibition. *Oncogene* **30**:3454–3467.

44. Zee C, P C, S D, MLJ A (1995) Imaging Features of Benign Gliomas. Benign Cerebral Glioma, pp. 247–274. American Association of Neurological Surgeons: Park Ridge, IL.

## SUPPORTING INFORMATION

Additional supporting information may be found in the online version of this article at the publisher's web site:

**Figure S1.** 3q26 genes SOX2 and OPA1 are targeted in glioma.

**Figure S2.** List of the oligonucleotides used in this report.

**Figure S3.** Data extracted from public databases.

**Figure S4.** SOX2 overexpression and OPA1 knock-down in LN319 alter cell proliferation.

**Figure S5.** Patient cohort.

**Table S6.** Characteristics of patients for statistical analysis.

**Table S7.** Coefficient estimates from tumor size parameters used to evaluate the oncogenic relevance of SOX2amp and OPA1del.

**Figure S8.** Tumor size parameters other than tumor necrosis volume used to evaluate the oncogenic relevance of SOX2amp and OPA1del.

**Table S9.** Impact of SOX2amp and OPA1del statuses on overall survival.